

## Synthesis of Silver Nanocomposite Hydrogel from Lysozyme-Mediated Poly(acrylamide) for the Inactivation of Pathogenic Bacteria

G. Viswanatha Reddy<sup>1,2</sup>, K. Madhusudana Rao<sup>3</sup>, K. S. V. Krishna Rao<sup>4\*</sup>, Chang-Sik Ha<sup>5\*</sup>

<sup>1</sup>Department of Chemistry, AP IIT, RK Valley, Idupulapaya – 516 330, India, <sup>2</sup>Department of Chemistry, Rayalaseema University, Kurnool – 518 007, India, <sup>3</sup>School of Chemical Engineering, Yeungnam University, 280 Daehak-Ro, Gyeongsan, Gyeongbuk - 38541, South of Korea, <sup>4</sup>Department of Chemistry, Polymer Biomaterial Design and Synthesis Laboratory, Yogi Vemana University, Kadapa – 516 003, Andhra Pradesh, India, <sup>5</sup>Department of Polymer Science and Engineering, Pusan National University, Gungjung-Gu, Busan-46241, Korea

### ABSTRACT

A simple eco-friendly method involving the lysozyme (Lys)-mediated controllable synthesis of silver nanoparticles (AgNPs) in poly(acrylamide) (PAAm) hydrogel networks is reported. The as-synthesized AgNPs present in the hydrogels were characterized by Fourier-transform infrared spectroscopy, UV-visible spectroscopy, X-ray diffraction, and scanning electron microscopy. Transmission electron microscopy and dynamic light scattering revealed the AgNPs to have a mean size of approximately 5–8 nm. The Lys-encapsulated hydrogel silver nanocomposite exhibited excellent antibacterial activity toward both Gram-positive and Gram-negative bacteria, which was superior to that of hydrogel silver nanocomposites produced by sodium borohydride reduction. The results highlight the potential of the Lys-mediated production of silver nanocomposites for antibacterial wound dressing applications.

**Key words:** Lysozyme, Hydrogel, Silver nanoparticles, Antibacterial activity, Wound dressing.

### 1. INTRODUCTION

Metal nanoparticles in hydrogels have a potential use in the catalysis, biomedical, and biotechnological fields [1,2]. The preparation of silver nanoparticles (AgNPs) in hydrogels is considered to be more attractive due to the controlled size and shape of AgNPs formed throughout the hydrogel network [3-10]. The size- and shape-controlled AgNPs in hydrogels have been used particularly for wound dressing purposes because of their antimicrobial activity against an extensive wide range of aerobic, anaerobic, Gram-negative, and Gram-positive bacteria [11]. Normally, hydrogels have been used as wound dressing materials in the form of tubes, dry sheets, and moist gel sheets. Hydrogel dressings are more advantageous because they can hydrate and maintain a moist wound bed as well as liquefy necrotic tissue [12]. These dressing materials can also promote the easier removal of necrotic tissue. Over the past few decades, numerous nano-silver-containing antimicrobial hydrogels have been reported [3-10]. Many studies have developed hydrogels using hydrophilic synthetic monomers and naturally occurring materials. Among them, poly(acrylamide) (PAAm) hydrogels composed of other synthetic polymers or natural carbohydrate materials have excellent ability to produce stable AgNPs [3-10].

The formation of size- and shape-controlled AgNPs in hydrogels depends on the type of material used to produce the hydrogels. Chemical, photoinduced, and microwave-assisted reduction methods are used generally to prepare AgNPs. The chemical reduction method is used most commonly to prepare stable AgNPs in hydrogel networks through equilibrium swelling (ES) in silver ion solutions followed by the reduction of the silver ions with reducing agents [3-8,10]. Despite these good results, the chemical reducing agents used for the reduction of metal ions in hydrogels are generally toxic and adversely affect the environment. Recently, a stable multicomponent system was also

used for the production of size- and shape-controlled AgNPs that were formed inside the hydrogel networks using sodium borohydride (NaBH<sub>4</sub>) as the reducing agent [10]. For environmental considerations, plant extracts have very recently been used for the synthesis of AgNPs in hydrogels [9,11]. Bimetallic nanoparticles were also developed in the hydrogel networks to enhance the antibacterial activity [10]. On the other hand, the combination of AgNPs with other materials with wound healing properties will be more convenient for enhancing the antibacterial activity.

Lysozyme (Lys) is an amphiphilic protein derived from hen egg white. Lys consists of a single polypeptide chain of 129 residues [13], in which 4.65% are lysine and 8.53% are arginine. These residues containing primary amines are strongly cationic proteins with isoelectric points at approximately pH 10.7. Lys is a well-recognized water-soluble antibacterial protein and has been used widely in food preservation, drug delivery, and biological applications [14,15]. Improved antibacterial activity had been reported when the conjugation of Lys with perillaldehyde and palmitic acid occurs [16,17]. The cationic nature and large amounts of amino acid residues present in Lys could reduce metal ions to metal nanoparticles [18,19].

### \*Corresponding author:

E-mail: ksvkr@yogivemanauniversity.ac.in

ISSN NO: 2320-0898 (p); 2320-0928 (e)

DOI: 10.22607/IJACS.2018.603010

Received: 22<sup>nd</sup> July 2018;

Revised: 26<sup>th</sup> July 2018;

Accepted: 26<sup>th</sup> July 2018

The present paper reports the synthesis of a PAAm-based silver nanocomposite hydrogel in the presence of Lys as an amphiphilic protein. Compared to previous reports, the present approach is simple for producing size- and shape-controlled AgNPs inside the networks without the use of chemical reducing agents or plant extracts and also without modification of the PAAm hydrogel [3-10]. This nanocomposite hydrogel is also expected to enhance the antibacterial properties due to the presence of both Lys and AgNPs in the hydrogel. To evaluate the antibacterial activity of the silver nanocomposite hydrogel, the hydrogel was applied to two different pathogenic bacteria, Gram-negative *Escherichia coli* and Gram-positive *Staphylococcus aureus*.

## 2. EXPERIMENTAL SECTION

### 2.1. Materials

Acrylamide (AAM), N,N'-methylenebisacrylamide (MBA), tetramethylethylenediamine (TEMED), potassium persulfate (KPS), sodium borohydride (NaBH<sub>4</sub>), silver nitrate (AgNO<sub>3</sub>), and Lys were purchased from Sigma-Aldrich. Double-distilled water was used throughout the experiment.

### 2.2. Synthesis of PAAm Hydrogels

PAAm hydrogel was synthesized using a simple traditional radical redox polymerization method. Briefly, 28.3 mM of AAM was dissolved in 7 mL of water. To this, 0.26 mM of MBA, 0.073 mM of KPS, and 1 mL of 1% TEMED were added. The hydrogels were formed under ambient conditions within 1 h. The hydrogels were then immersed in water for 2 days to remove the unreacted monomers, and the other chemicals were removed by changing the water every 12 h. The hydrogels were dried at 40°C in a hot air oven to reach a constant weight. The hydrogel was stored in a desiccator for further study.

### 2.3. Synthesis of Antibacterial Hydrogels

**Lys-PAAm-Ag<sup>0</sup> hydrogel:** To prepare the Lys-PAAm-Ag<sup>0</sup> hydrogel, the dried PAAm hydrogel was equilibrated in a large amount of water for 2 days to reach ES. The swollen hydrogel was transferred to a 250 mL beaker containing 50 mL of 5mM AgNO<sub>3</sub> solution to allow the maximum silver ions to infiltrate the hydrogel networks. The hydrogel was removed from the AgNO<sub>3</sub> solution and washed with distilled water to remove surface adhered silver salts. The silver ion-loaded hydrogel was transferred to a 100 mL beaker containing 50 mL of a 0.5% Lys aqueous solution and kept for 24 h for the reduction of silver ions to AgNPs in the hydrogel networks. Lys was also encapsulated in the hydrogel networks to stabilize the AgNPs formed. The hydrogel nanocomposite was dried at ambient temperature to reach a constant weight.

**Lys-PAAm:** The PAAm hydrogel was soaked in 100 mL beaker containing 50 mL of a 0.5% Lys solution for 2 days to absorb the maximum amount of Lys in the hydrogel networks. The hydrogels were air dried to a constant weight.

**PAAm-Ag<sup>0</sup>:** The same procedure was used to load the silver ions into the PAAm hydrogel as described for the synthesis of Lys-PAAm-Ag<sup>0</sup>. The silver ion-loaded PAAm hydrogel was placed into a beaker containing 50 mL of a 5 mM cold NaBH<sub>4</sub> solution for 6 h to reduce the silver ions to AgNPs. The composite hydrogel was dried at 40°C to reach a constant weight.

### 2.4. Characterization

Fourier-transform infrared (FTIR) spectroscopy of the samples was performed using a JASCO (FTIR-4100) spectrometer. The samples

were finely grounded with KBr to prepare pellets under a hydraulic pressure of 600 dynes/cm<sup>2</sup>, and the spectra were scanned in the range of 4000–400 cm<sup>-1</sup>. UV-visible spectra of the silver nanocomposite hydrogels (10 mg in 10 mL of distilled water) were obtained using a HITACHI U-2010 UV-visible spectrophotometer. X-ray diffraction (XRD, Rigaku mini field goniometer) was performed using Cu-K $\alpha$  radiation ( $\lambda=1.5418 \text{ \AA}$ ) at 30 kV and 40 mA over the range, 1.2–50° 2 $\theta$ . Thermogravimetric analysis (TGA, Perkin-Elmer Pyris Diamond TG) was performed at a heating rate of 10°C min<sup>-1</sup> in air (30–800°C). The morphological variations of the hydrogel and hydrogel nanocomposites were examined by scanning electron microscopy (SEM Table-top mini, SNE-3000M). High-resolution transmission electron microscopy (HR-TEM, JEOL JEM-2010) was performed at an accelerating voltage of 200 kV. The samples were prepared by dropping 5–10  $\mu$ L of finely ground nanocomposite hydrogel dispersions onto a copper grid and dried at room temperature after removing the excess moisture with filter paper.

### 2.5. Swelling Studies

Swelling studies of the hydrogel and silver nanocomposite hydrogels were performed in water at room temperature. First, the dried hydrogel samples were weighed and soaked in water for 2 days. After reaching equilibrium, the hydrogel and silver nanocomposite hydrogels were removed from water and blotted carefully with a wiper to remove the surface adhered water and then weighed. The ES ratio (%ES) of the hydrogel was calculated using the following equation:

$$\%ES = \left[ \frac{W_e - W_d}{W_d} \right] \quad (1)$$

Where  $W_e$  is the weight of swollen hydrogel and  $W_d$  is the weight of the dry hydrogel.

### 2.6. Antibacterial Activity of Hydrogels

Both Gram-positive *S. aureus* and Gram-negative *E. coli* were cultivated at 37°C in a sterilized Luria-Bertani (LB) broth (peptone 10 g, yeast extract 5 g, NaCl 10 g, and distilled water 1000 mL) at 150 rpm in a shaker for 16 h. An antibacterial study of the silver nanocomposite hydrogel was carried out using the paper disc method. Briefly, 50  $\mu$ L of bacteria medium ( $10^5$ – $10^6$  colony-forming unit [CFU] mL<sup>-1</sup>) was dispensed on an agar plate. A 10 mg/10 mL sample of the nanocomposite hydrogel solutions was prepared in distilled water and 50  $\mu$ L of the test solution was added to the discs. The plates were then incubated for 24 h at 37°C. The inhibition zone appearing around the disc was measured and recorded.

The kinetics of the bacterial growth inhibition ratio of hydrogels was studied using the LB broth method. 0.3 g of the hydrogel samples were immersed in 100 mL of sterile Erlenmeyer flasks containing 40 mL of a germ-containing nutrient solution with a  $10^5$ – $10^6$  CFU mL<sup>-1</sup> bacterial concentration. The pure bacteria medium ( $10^5$ – $10^6$  CFU mL<sup>-1</sup>) was also incubated and used as a control. All flasks were incubated at 37°C and 150 rpm for 48 h. Bacterial growth was measured at 600 nm using a spectrophotometer. All the experiments were conducted in triplicate to determine the standard deviation. The inhibition ratios for all samples were calculated as follows:

$$\text{Inhibition ratio (\%)} = 100 - 100 \times \frac{[A_t - A_0]}{[A_{con} - A_0]} \quad (2)$$

Where  $A_0$  is the optical density (OD) for the bacterial broth medium before incubation, and  $A_t$  and  $A_{con}$  are the ODs of the nanocomposite and control sample after incubation, respectively.

### 3. RESULTS AND DISCUSSIONS

#### 3.1. Synthesis of AgNPs in Poly(AAm) Hydrogels

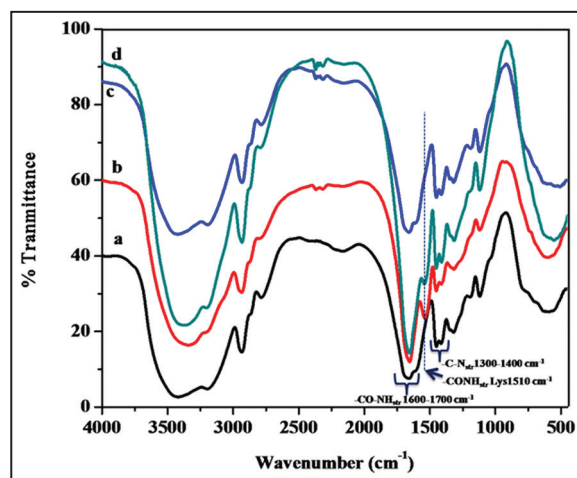
In general, more stable AgNPs are formed when the hydrogels contain more hydrophilic units, such as  $-OH$ ,  $-CONH_2$ ,  $-COOH$ , and  $NH_2$ . These hydrophilic groups are responsible for anchoring the silver ions in aqueous solutions. Many studies used modified PAAm hydrogels as templates for the formation of more stable and size-controlled AgNPs using chemical reducing agents and plant extracts [3-11]. The formation, stability, and controllable size depend on the modification of PAAm with other synthetic or natural polymers. In the present contribution, AgNPs with a highly controllable and uniform size and shape were fabricated using protein-mediated approach without modified PAAm hydrogel networks. In this study, Lys was used to reduce the silver ions in the gel networks. First silver ions were anchored through coordination with the amide functionality of hydrogel networks. The anchored silver ions could be reduced easily inside the hydrogel networks by Lys because of its reducing property [18,19]. More importantly, the AgNPs were highly stable in the hydrogel networks because of the electrostatic interactions between Lys and AgNPs. Scheme 1 shows a schematic diagram of the formation of AgNPs in the hydrogels. The formation, thermal, and morphological properties of synthesized nanocomposite hydrogels are discussed in the subsequent sections.

#### 3.2. Characterization

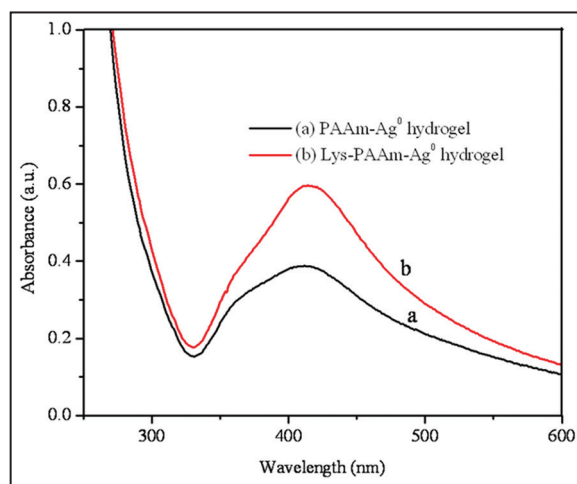
The formation of hydrogel was confirmed by FTIR spectral analysis. Figure 1 shows the FTIR spectra of (a) PAAm hydrogel, (b) Lys-loaded PAAm hydrogel, (c) PAAm-Ag<sup>0</sup> composite hydrogel after NaBH<sub>4</sub> reduction, and (d) PAAm-Ag<sup>0</sup> composite hydrogel after Lys reduction. For the pure PAAm hydrogel, the characteristic peaks were observed in the range, 1600–1700 cm<sup>-1</sup>, which were assigned to C=O groups. A broad absorption band at 3200–3500 cm<sup>-1</sup> was attributed to N-H stretching vibrations. The characteristic peaks belonging to the C-N and C-H stretching vibrations were observed at 1300–1400 cm<sup>-1</sup> and 2950 cm<sup>-1</sup>, respectively. The Lys-PAAm hydrogel showed a new band at 1510 cm<sup>-1</sup> due to the  $-CONH-$  band of the Lys protein. In the case of the silver composite hydrogel, all the bands were shifted slightly to a lower frequency, indicating the interactions between the hydrogel chains with AgNPs.

The AgNPs embedded in the hydrogel networks were tested by UV-Vis spectral analysis (Figure 2). The prepared aqueous solutions of the PAAm-Ag<sup>0</sup> hydrogel (a) showed a broad absorption band at 415 nm, which was assigned to the surface plasmon resonance band of formed AgNPs. The broad UV spectra indicated that the synthesized AgNPs are not uniform in nature. In contrast, the PAAm-Ag<sup>0</sup> composite hydrogel (b) showed a symmetrical UV peak around 420 nm, indicating the formation of highly controlled and uniform AgNPs. Therefore, Lys could not only control the formation of AgNPs but also promote their stabilization in PAAm hydrogels to a greater extent compared to other published reports [5-11]. The formation of AgNPs was verified further by XRD. Figure 3 shows the XRD patterns of (a) pure PAAm, (b) PAAm-Ag<sup>0</sup>, (c) Lys-PAAm, and (d) Lys-PAM-Ag<sup>0</sup>. The peaks at

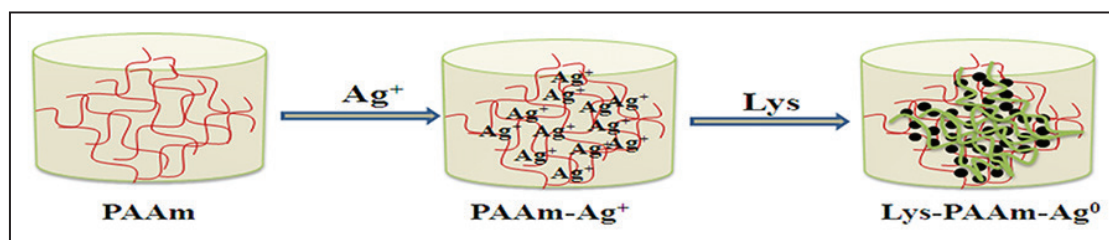
38°, 44°, 64°, and 78° 2 $\theta$  for both the PAAm-Ag<sup>0</sup> and Lys-PAAm-Ag<sup>0</sup> hydrogels showed crystalline properties. The crystalline peaks were assigned to the (111), (200), (220), and (311) planes of Ag, which suggests highly crystalline AgNPs with a face-centered cubic structure (FCC) were formed in the hydrogels using both NaBH<sub>4</sub> and Lys. The formation of crystalline, nanostructured AgNPs in hydrogel networks is quite common [3-8, 10]. Sharp and intense peaks represent the highly crystalline silver nanostructures formed in the hydrogel networks with Lys reduction. In the pure PAAm hydrogel and Lys-PAAm hydrogel, however, no such peaks were observed because of the amorphous nature of the hydrogels.



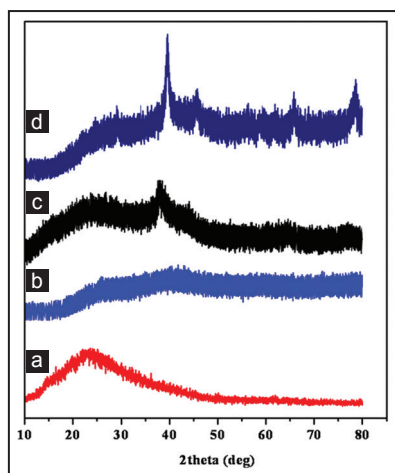
**Figure 1:** Fourier-transform infrared spectra of (a) poly(acrylamide) (PAAm), (b) lysozyme (Lys)-PAAm, (c) PAAm-Ag<sup>0</sup>, and (d) Lys-PAAm-Ag<sup>0</sup> hydrogels.



**Figure 2:** UV-visible spectra of (a) poly(acrylamide) (PAAm)-Ag<sup>0</sup> and (b) lysozyme (Lys)-PAAm-Ag<sup>0</sup> hydrogels.



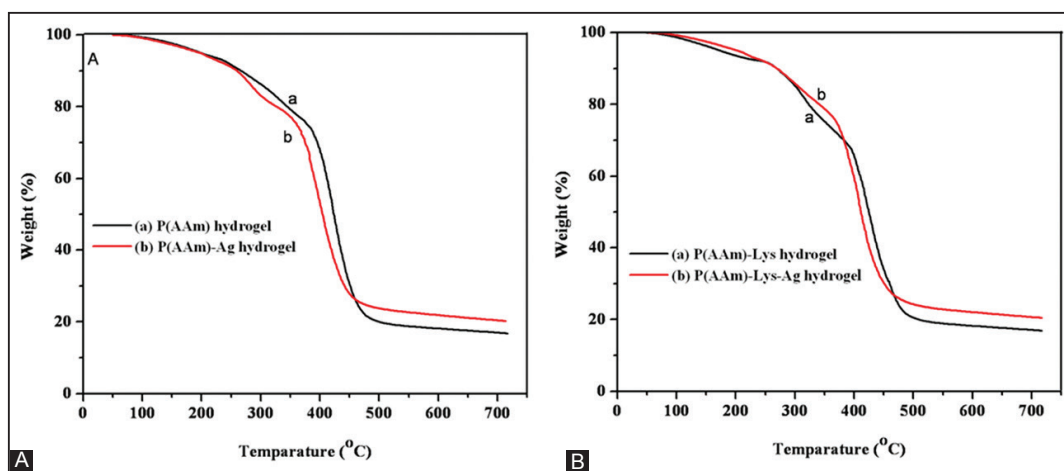
**Scheme 1:** Schematic representation of the formation of lysozyme-poly(acrylamide)-Ag<sup>0</sup> hydrogels.



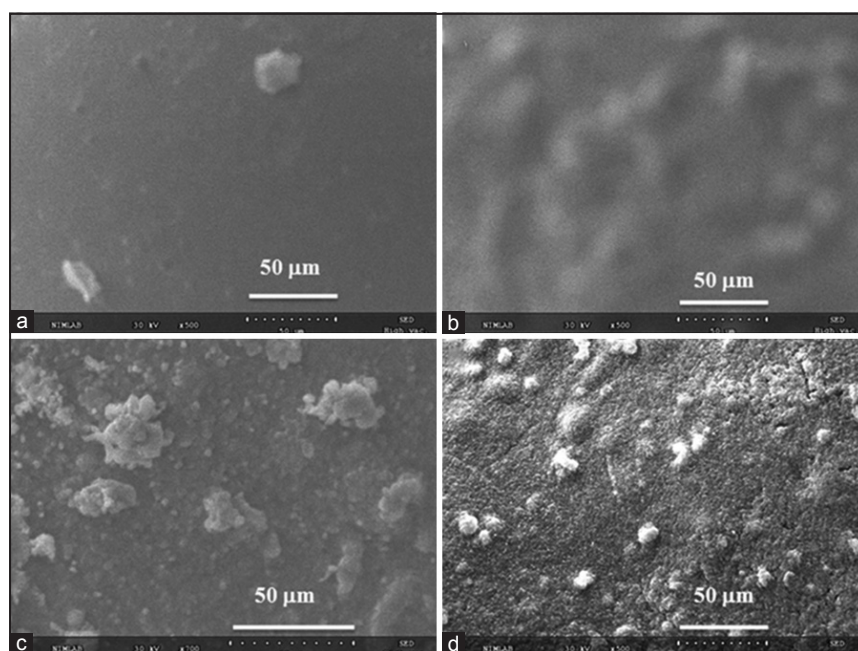
**Figure 3:** X-ray diffraction patterns of (a) poly(acrylamide) (PAAm), (b) lysozyme (Lys)-PAAm, (c) PAAm-Ag<sup>0</sup>, and (d) Lys-PAAm-Ag<sup>0</sup> hydrogels.

Figure 4 shows the TGA curves of the hydrogel and silver nanocomposites. The weight loss observed in the case of the PAAm hydrogel was 79% at 490°C, whereas the weight loss for PAAm-Ag<sup>0</sup> composite was 65%. This indicates the excellent thermal properties of the composite hydrogel due to the presence of AgNPs. A similar thermal property was observed for Lys-PAAm-Ag<sup>0</sup>, indicating that Lys has similar reduction properties to NaBH<sub>4</sub>. The weight loss difference between the pristine PAAm and PAAm-Ag<sup>0</sup> composite hydrogel was 9%. A similar weight loss difference was also observed in the case of the Lys-PAAm and Lys-PAAm-Ag<sup>0</sup> composite hydrogels.

Figure 5 shows SEM images of the surface morphology of the hydrogel and composite hydrogels. The surface morphology of the pure PAAm hydrogel (a) and Lys-PAAm hydrogel (b) showed a smooth surface. On the other hand, a clear change in surface morphology was observed for the PAAm-Ag<sup>0</sup> (c) and Lys-PAAm-Ag<sup>0</sup> (d) composite hydrogels. The individual AgNPs were observed for PAAm-Ag<sup>0</sup>. The surface morphology of Lys-PAAm-Ag<sup>0</sup> did not show individual AgNPs because the AgNPs were covered by the amphiphilic protein through



**Figure 4:** Thermogravimetric analysis curves of (A): (a) Poly(acrylamide) (PAAm) and (b) PAAm-Ag<sup>0</sup>, and (B): (a) Lysozyme (Lys)-PAAm and (b) Lys-PAAm-Ag<sup>0</sup> hydrogels.



**Figure 5:** Scanning electron microscopy images of (a) poly(acrylamide) (PAAm), (b) lysozyme (Lys)-PAAm, (c) PAAm-Ag<sup>0</sup>, and (d) Lys-PAAm-Ag<sup>0</sup> hydrogels.

strong electrostatic interactions. The morphology and size distribution of the AgNPs present in the hydrogel networks were determined by TEM and dynamic light scattering (DLS) studies, as shown in Figures 6 and 7. In Figure 6, the PAAm-Ag<sup>0</sup> nanocomposite hydrogel (a and b) showed different sizes of AgNPs with a spherical morphology. TEM of the Lys-PAAm-Ag<sup>0</sup> composite (d and e) showed that spherical AgNPs (mean diameter of 5–8 nm) were formed throughout the hydrogel networks without agglomeration. A similar morphology was reported after the modification of PAAm hydrogels with other natural or synthetic polymers using NaBH<sub>4</sub> or plant extracts as the reducing agents [3-11]. In the present study, the presence of Lys can explain the formation of stably distributed, discrete AgNPs in the PAAm hydrogels without agglomeration. The selective diffraction pattern of the AgNPs revealed (111), (200), (220), (311), and (222) peaks in the three diffraction patterns for both PAAm-Ag<sup>0</sup> and Lys-PAAm-Ag<sup>0</sup> (c and f, respectively), confirming the FCC structure of the AgNPs. DLS results of AgNPs in (a) PAAm-Ag<sup>0</sup> and (b) Lys-PAAm-Ag<sup>0</sup> also confirmed the size of AgNPs (Figure 7). The reduction of silver ions in the hydrogel networks with NaBH<sub>4</sub> produced a bimodal distribution curve with two distinguishable sizes, 2 nm and 18 nm. Lys reduction produced a narrow unimodal distribution, 5–8 nm in size, because Lys could control the particle size and shape during the formation of AgNPs in the hydrogels.

### 3.3. Swelling Results

Table 1 lists the ES ratios (%ES) of the PAAm hydrogels and Ag<sup>0</sup>-loaded PAAm hydrogels. The PAAm hydrogel showed an ES value of 369±4%. A similar type of swelling was observed in the case of Lys-PAAm due to the release of Lys from the PAAm hydrogel during the

swelling of the hydrogel. On the other hand, the swelling was increased for the Ag<sup>0</sup>-loaded hydrogel. The presence of AgNPs embedded in the hydrogel caused an enlargement of the hydrogel networks. The significant increase in the degree of hydration was attributed to the presence of a surface charge on the Ag colloidal nanoparticles [4].

### 3.4. Anti-bacterial Properties of Hydrogels

Silver nanomaterials are used most widely in medicine because of their antibacterial action on different pathogenic bacteria. AgNPs easily interfere with the respiratory chain at the cytochromes [20] or interfere with the components of the microbial electron transport system, binding DNA and inhibiting DNA replication [21]. The antibacterial activity depends on the size and stability of the AgNPs. The smaller size and higher stability of AgNPs promote higher antibacterial activity for both Gram-positive and negative bacteria. As the size decreases, however, there are a larger number of atoms on the

**Table 1:** % ES and the average inhibition zones for hydrogels

| Sample code              | %ES±SD | <i>E. coli</i><br>(cm±SD) | <i>S. aureus</i><br>(cm±SD) |
|--------------------------|--------|---------------------------|-----------------------------|
| PAAm                     | 326±4  | NA                        | NA                          |
| Lys-PAAm                 | 321±2  | NA                        | 0.3±0.02                    |
| PAAm-Ag <sup>0</sup>     | 339±5  | 0.8±0.06                  | 0.7±0.01                    |
| Lys-PAAm-Ag <sup>0</sup> | 342±2  | 0.9±0.2                   | 1.2±0.1                     |

NA: Not appearing, SD: Standard deviation. ES: Equilibrium swelling, *E. coli*: *Escherichia coli*, *S. aureus*: *Staphylococcus aureus*, PAAm: Poly (acrylamide), Lys: Lysozyme

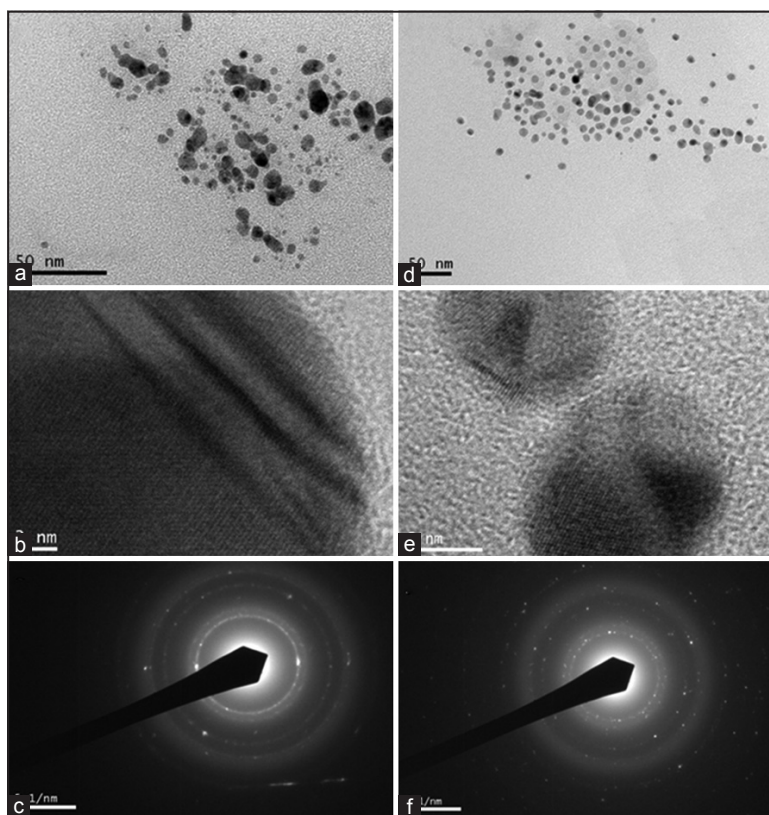


**Figure 6:** High-resolution transmission electron microscopy images of silver nanoparticles in poly(acrylamide) (PAAm)-Ag<sup>0</sup> (a and b) and lysozyme (Lys)-PAAm-Ag<sup>0</sup> hydrogels (d and e), where (a) and (d) are in low magnification, while (b) and (e) are in high magnification. The ED patterns of silver nanoparticles in PAAm-Ag<sup>0</sup> and Lys-PAAm-Ag<sup>0</sup> hydrogels are also shown in (c) and (f), respectively.

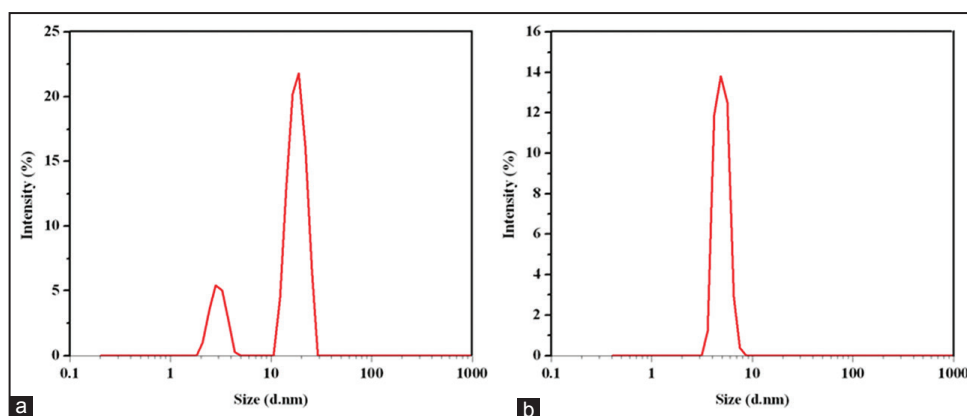


**Figure 7:** Dynamic light scattering particle size distribution curves of silver nanoparticles (AgNPs) in (a) poly(acrylamide) (PAAm)-Ag<sup>0</sup> and (b) lysozyme-PAAm-Ag<sup>0</sup> hydrogels.

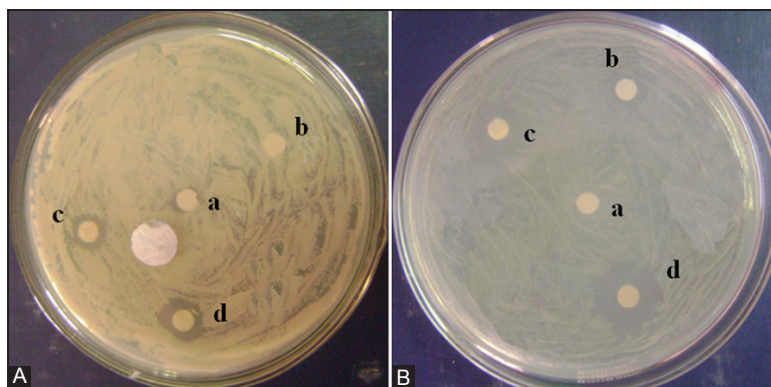


**Figure 8:** Antibacterial activity images of silver nanocomposite hydrogels against (A) *Escherichia coli*, and (B) *Staphylococcus aureus* for (a) poly(acrylamide) (PAAm), (b) lysozyme (Lys)-PAAm, (c) PAAm-Ag<sup>0</sup>, and (d) Lys-PAAm-Ag<sup>0</sup>.

surface available to interact with bacteria or release a larger number of silver ions. Higher stability produces better antibacterial properties. Unstable nanoparticles tend to form aggregates, which would reduce the surface area and the density of atoms available on the surface [22]. The antibacterial activity of all hydrogel and silver nanocomposite hydrogels was evaluated by measuring the inhibition zone against two important pathogenic bacteria, *E. coli* and *S. aureus* (Figure 8). Table 1 lists the measured antibacterial inhibition zones for all samples. The Lys-PAAm-Ag<sup>0</sup> composite exhibited higher antibacterial activity on both *E. coli* and *S. aureus* because of the presence of a smaller size of AgNPs in the hydrogels with higher stability. High antibacterial activity was observed on *S. aureus* due to Lys, which deactivates bacterial growth. This can be explained based on the proportions of peptidoglycan available on the bacteria cell walls. Lys hydrolyzes  $\beta(1\rightarrow4)$  linkages between *N*-acetylmuramic acid and the *N*-acetyl-D-glucosamine residues in peptidoglycan and between the *N*-acetyl-D-glucosamine residues in chitodextrin. Gram-positive cells are quite susceptible to this type of hydrolysis because their cell walls have a high proportion of peptidoglycan. Gram-negative bacteria are less susceptible due to the presence of an outer membrane and a smaller proportion of peptidoglycan.

The quantitative antibacterial effect of the composite hydrogels was studied on both *E. coli* and *S. aureus* using the LB broth method. In this method, quantitative determination of the antibacterial activity is expressed in terms of the % inhibition ratio (Figure 9). The PAAm hydrogel did not show an inhibition ratio, whereas PAAm-Lys, PAAm-Ag<sup>0</sup>, and Lys-PAAm-Ag<sup>0</sup> showed a certain inhibition ratio. Lys-PAAm-Ag<sup>0</sup> showed the highest inhibition ratio among all hydrogels.

The inhibition ratio was decreased after 24 h for PAAm-Ag<sup>0</sup>. This is because the maximum amount of AgNPs was involved in inhibiting bacterial growth up to 24 h. After that, there were no AgNPs available to kill the bacteria. Therefore, the bacteria grew again after 24 h. For Lys-PAAm-Ag<sup>0</sup>, there was no change in the inhibition ratio even up to 48 h. Owing to the longtime release of AgNPs from the hydrogels, Lys could act as a stabilizer to control the release of AgNPs and inhibit bacterial growth. Therefore, this design of the AgNP-embedded hydrogel has great potential due to its highest antibacterial activity. Bacteria are one of the main reasons for the reducing healing property of colonized and infected wounds, which cause discomfort to the patient, and possibly cause life-threatening illness. Silver possesses antibacterial activity to suspend bacterial growth. Therefore, silver can be used as an antibacterial wound dressing material. These results show that Lys plays an important role not only in the reduction of size-controlled AgNPs but also in stabilizing the AgNPs in hydrogels with improved antibacterial activity on both Gram-positive and Gram-negative pathogenic bacteria. Therefore, these new types of Lys-PAAm-Ag<sup>0</sup> composites can be applied potentially for wound dressing antibacterial applications.

#### 4. CONCLUSIONS

Highly controllable AgNPs in PAAm hydrogels were developed using Lys for protein-mediated synthesis. The highly uniform size and shape of the AgNPs were regulated to 5–8 nm by the Lys chains available throughout the hydrogel. Therefore, the Lys would be highly efficient for the formation of AgNPs and as a stabilizer in the hydrogels. The developed hydrogel silver nanocomposite exhibited excellent

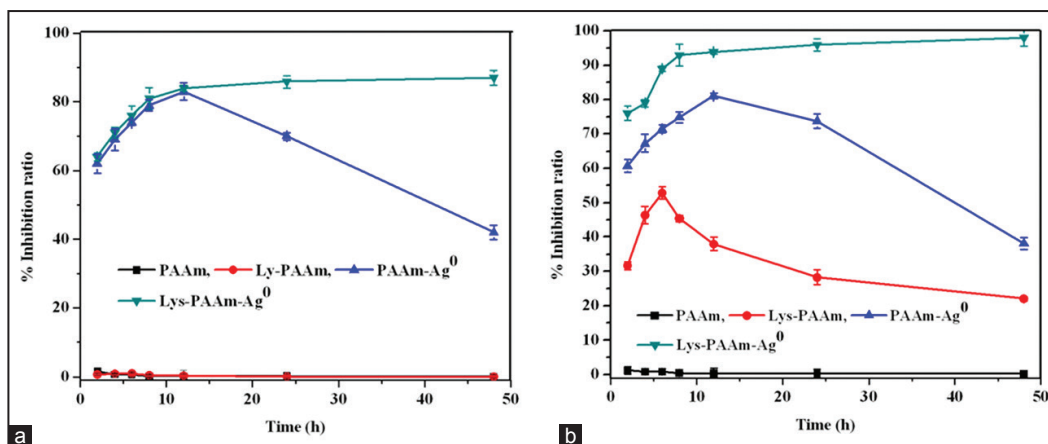


**Figure 9:** Antibacterial activity inhibition ratio kinetic curves of (a) *Escherichia coli*, and (b) *Staphylococcus aureus* for hydrogels and silver nanocomposite hydrogels.

antibacterial activity toward two different pathogenic bacteria. Overall, these results confirm the synthesis of a new type of composite hydrogel with potential wound dressing applications.

## 5. ACKNOWLEDGMENTS

The work was supported by the National Research Foundation of Korea (NRF) Grant funded by the Ministry of Science, ICT and Future Planning, Korea. (Acceleration Research Program (NRF-2014 R1A2A111 054584) and Brain Korea 21 Plus Program (21A2013800002)).

## 6. REFERENCES

1. S. Butun, N. Sahiner, (2011) A versatile hydrogel template for metal nano particle preparation and their use in catalysis, *Polymer*, **52**: 4834-4840.
2. A. K. Gaharwar, N. A. Peppas, A. Khademhosseini, (2014) Nanocomposite hydrogels for biomedical applications, *Biotechnology and Bioengineering*, **11**: 441-449.
3. P. S. K. Murthy, Y. M. Mohan, K. Varaprasad, B. Sreedhar, K. M. Raju, (2008) First successful design of semi-IPN hydrogel-silver nanocomposites: A facile approach for antibacterial application, *Journal of Colloid and Interface Science*, **318**: 217-224.
4. Y. M. Mohan, K. Vimala, V. Thomas, K. Varaprasad, B. Sreedhar, (2010) Controlling of silver nanoparticles structure by hydrogel networks, *Journal of Colloid and Interface Science*, **342**: 73-84.
5. Y. Kim, V. R. Babu, D. T. Thangadurai, K. S. V. K. Rao, H. Cha, C. Kim, W. Joo, Y. I. Lee, (2011) Synthesis, characterization, and antibacterial applications of novel copolymeric silver nanocomposite hydrogels, *Bulletin of the Korean Chemical Society*, **32**: 553-558.
6. S. Park, P. S. K. Murthy, S. Park, Y. M. Mohan, W. G. Koh, (2011) Preparation of silver nanoparticle-containing semi-interpenetrating network hydrogels composed of pluronic and poly(acrylamide) with antibacterial property, *Journal of Industrial and Engineering Chemistry*, **17**: 293-297.
7. K. Varaprasad, Y. M. Mohan, S. Ravindra, N. N. Reddy, K. Vimala, K. Monika, B. Sreedhar, K. Mohana Raj, (2010) Hydrogel-silver nanoparticle composites: A new generation of antimicrobials, *Journal of Applied Polymer Science*, **115**: 1199-1207.
8. H. Cha, V. R. Babu, K. S. V. K. Rao, Y. Kim, S. Mei, W. H. Joo, Y. I. Lee, (2012) Fabrication of amino acid based silver nanocomposite hydrogels from pva-poly (Acrylamide-co-Acryloyl phenylalanine) and their antimicrobial studies, *Bulletin of the Korean Chemical Society*, **33**: 3191-3195.
9. S. Siraj, K. M. Rao, P. Sudhakar, A. Chandrababu, G. J. Mohiddin, K. C. Rao, M. C. S. Subha, (2013) A green approach to synthesize silver nanoparticles in starch-co-poly(acrylamide) hydrogels by *Tridax procumbens* Leaf extract and their antibacterial activity, *International Journal of Carbohydrate Chemistry*, **539636**: 1.
10. K. M. Rao, K. S. V. K. Rao, G. Ramanjaneyulu, K. C. Rao, M. C. S. Subha, C. S. Ha, (2014) Biodegradable sodium alginate-based semi-interpenetrating polymer network hydrogels for antibacterial application, *Journal of Biomedical Materials Research Part A*, **102A**: 3196-3206.
11. B. Manjula, K. Varaprasad, R. Sadiku, K. Ramam, G. V. S. Reddy, K. M. Raju, (2014) Development of microbial resistant thermosensitive Ag nanocomposite (gelatin) hydrogels via green process, *Journal of Biomedical Materials Research Part A*, **102A**: 928-934.
12. K. Varaprasad, G. S. M. Reddy, J. Jayaramudu, R. Sadiku, K. Ramama, S. S. Ray, (2014) Development of microbial resistant carbopol nanocomposite hydrogels via a green process, *Biomaterials Science*, **2**: 257-263.
13. C. C. F. Blake, D. F. Koenig, G. A. Mair, A. C. T. North, D. C. Phillips, V. R. Sarma, (1965) Structure of hen egg-white lysozyme: A three-dimensional Fourier synthesis at 2 Å resolution, *Nature*, **206**: 757-761.
14. K. Zhu, T. Ye, J. Liu, Z. Peng, S. Xu, J. Lei, H. Deng, B. Li, (2013) Nanogels fabricated by lysozyme and sodium carboxymethyl cellulose for 5-fluorouracil controlled release, *International Journal of Pharmaceutics*, **441**: 721-727.
15. N. Charemsriwilaiwat, P. Opanasopit, T. Rojanarata, T. Ngawhirunpat, (2012) Lysozyme-loaded, electrospun chitosan-based nanofiber mats for wound healing, *International Journal of Pharmaceutics*, **427**: 379-384.
16. H. Ibrahim, R. Hatta, M. Fujiki, M. Kim, T. Yamamoto, (1994) Enhanced antimicrobial action of lysozyme against gram negative bacteria due to modification with perillaldehyde, *Journal of Agricultural and Food Chemistry*, **42**: 1813-1817.
17. S. Nakamura, Y. Gohya, J. N. Losso, S. Nakai, A. Kato, (1996)

- Protective effect of lysozyme-galactomannan or lysozyme-palmitic acid conjugates against *Edwardsiella tarda* infection in carp. *Cyprinus carpio* L, *FEBS Letters*, **383**: 251-254.
18. K. Qu, L. Wu, J. Ren, X. Qu, (2013) Enzyme-directed pH-responsive exfoliation and dispersion of graphene and its decoration by gold nanoparticles for use as a hybrid catalyst, *Nano Research*, **6**: 693-702.
  19. D. M. Eby, N. M. Schaeublin, K. E. Farrington, S. M. Hussain, G. R. Johnson, (2009) Lysozyme catalyzes the formation of antimicrobial silver nanoparticles, *ACS Nano*, **3**: 984-994.
  20. S. Prabhu, E. K. Poulse, (2012) Silver nanoparticles: mechanism of antimicrobial action, synthesis, medical applications, and toxicity effects, *International Nano Letters*, **32**: 1-10.
  21. K. Kon, M. Rai, (2013) Metallic nanoparticles: Mechanism of antibacterial action and influencing factors, *Journal of Comparative Pathology*, **2**: 160-174.
  22. C. M. Jones, E. M. V. Hoek, (2010) A review of the antibacterial effects of silver nanomaterials and potential implications for human health and the environment, *Journal of Nanoparticle Research*, **12**: 1531-1551.